GEOLOGY | THE GEOLOGICAL SOCIETY OF AMERICA®

https://doi.org/10.1130/G48759.1

Manuscript received 22 December 2020
Revised manuscript received 9 April 2021
Manuscript accepted 13 April 2021

Published online 14 June 2021

Slab-derived sulfate generates oxidized basaltic magmas in the southern Cascade arc (California, USA)

Michelle J. Muth and Paul J. Wallace
Department of Earth Sciences, University of Oregon, Eugene, Oregon 97403-1272, USA

ABSTRACT

Whether and how subduction increases the oxidation state of Earth's mantle are two of the most important unresolved questions in solid Earth geochemistry. Using data from the southern Cascade arc (California, USA), we show quantitatively for the first time that increases in arc magma oxidation state are fundamentally linked to mass transfer of isotopically heavy sulfate from the subducted plate into the mantle wedge. We investigate multiple hypotheses related to plate dehydration and melting and the rise and reaction of slab melts with mantle peridotite in the wedge, focusing on electron balance between redox-sensitive iron and sulfur during these processes. These results show that unless slab-derived silicic melts contain much higher dissolved sulfur than is indicated by currently available experimental data, arc magma generation by mantle wedge melting must involve multiple stages of mantle metasomatism by slab-derived oxidized and sulfur-bearing hydrous components.

INTRODUCTION

Over long time scales, recycling of redox-sensitive sulfur (S) in subduction zones is likely a key control on the oxidation state of Earth's mantle (Evans, 2012). The redox state of arc magmas also strongly affects their chemical evolution and the creation of porphyry ore deposits (Richards, 2015). In arc magmas, S is present both as sulfide (S^{2-}), the dominant species in mid-ocean ridge basalt (MORB), and as the oxidized species sulfate (S^{6+}). Trace element systematics suggest that arc magmas become oxidized and S^{6+} dominated during differentiation (Lee et al., 2010; Tang et al., 2018). In contrast, data from mantle xenoliths and from redox state measured in silicate glasses (Kelley and Cottrell, 2009; Brounce et al., 2014; Birner et al., 2017; Bénard et al., 2018) suggest oxidized magmas form when oxidized materials from the downgoing slab rise into the sub-arc mantle wedge.

Independent of this debate, $\delta^{34}S$ values measured in arc glasses and volcanic gases suggest that some S is derived from seawater sulfate released during slab dehydration (Alt et al., 1993; Bénard et al., 2018). Although mantle melts contain much less S than Fe, one mole of slab-derived S^{6+} can potentially oxidize eight moles of Fe^{2+}. Whether this S^{6+}-driven oxidation occurs in arcs is difficult to test because it requires integrating the mass transfer of S and electron budget of S and Fe into models of magma formation.

Olivine-hosted melt inclusions (MIs) provide a means to study melts minimally affected by degassing. We measured the composition of MIs hosted in Mg-rich olivine from tephra of six mafic cinder cones in the Lassen segment of the Cascade arc, California (USA). This region has hundreds of mafic vents that have been variably influenced by slab-derived material in their mantle source (Borg et al., 1997). Lassen sits at the southern end of the Cascadia subduction zone, which has a hotter thermal structure than most arcs (Syracuse et al., 2010). Water in Lassen magmas is likely derived from dehydration of hydrated mantle lithosphere in the subducting Gorda microplate, with the released fluid fluxing into overlying oceanic crust where it induces slab melting (Walowski et al., 2015, 2016). We build on this framework, constraining the mass balance and source of S in Lassen magmas using microanalysis of $\delta^{34}S$, S, and Sr/Nd in the same MIs for which we constrain electron balance using $S^{6+}/\sum S$ and $Fe^{3+}/\sum Fe$ values measured via X-ray absorption near edge structure (XANES) spectroscopy (see the Supplemental Material[1] for details of all analytical methods).

SLAB-DERIVED SULFUR

Arc magmas commonly contain more S than MORB does, regardless of subducted-plate thermal structure (Fig. 1). After corrections for post-entrapment crystallization, average S contents in MIs for Lassen cinder cones range from 990 ± 160 ppm (cinder cone BBL), similar to primitive MORB values, to 1960 ± 470 ppm (cinder cone BRM). Within each cone, MIs do not show signs of S degassing (Figs. S4B and S12 in the Supplemental Material). To compare conditions of melting that generated magmas at each cone, we calculated primary magma compositions through olivine addition back to equilibrium with Fo_{90} (where Fo indicates forsterite content) olivine. Primary magma S contents, thus calculated, range from 790 to 1940 ppm (Fig. S12; see the Supplemental Material).

To assess the influence of slab-derived S on Lassen primary magma S contents, we compared S/Dy to Sr/Nd. Sr and Nd, and S and Dy, respectively, have similar incompatibility during mantle melting in the presence of immiscible sulfides and during olivine-only fractional crystallization (Saal et al., 2002; Walowski et al., 2016). This means increases in Sr and/or S relative to Nd and/or Dy can indicate addition of slab material to the mantle source. Increases in S/Dy can also indicate more oxidized melting conditions, which increase the maximum S content of sulfide-saturated melts.

The S/Dy ratio correlates with Sr/Nd at Lassen (Fig. 2D). If we make a simplifying assumption that relationships between S/Dy and Sr/Nd are linear, a regression including an averaged value for MORB data yields $R^2 = 0.69$ and p-value $= 0.02$. We note that cinder cone BRVB is an outlier to this correlation and attribute this to preexisting enrichments in Nd within the sub-arc mantle prior to modern subduction (see the Supplemental Material text and Figs. S14 and S15). Correlations with

[1]Supplemental Material. Tables S1–S14, Figures S1–S16, and supplemental methods. Please visit https://doi.org/10.1130/GEOL.S.14699628 to access the supplemental material, and contact editing@geosociety.org with any questions.

CITATION: Muth, M.J., and Wallace, P.J., 2021, Slab-derived sulfate generates oxidized basaltic magmas in the southern Cascade arc (California, USA): Geology, v. 49, p. 1177–1181, https://doi.org/10.1130/G48759.1

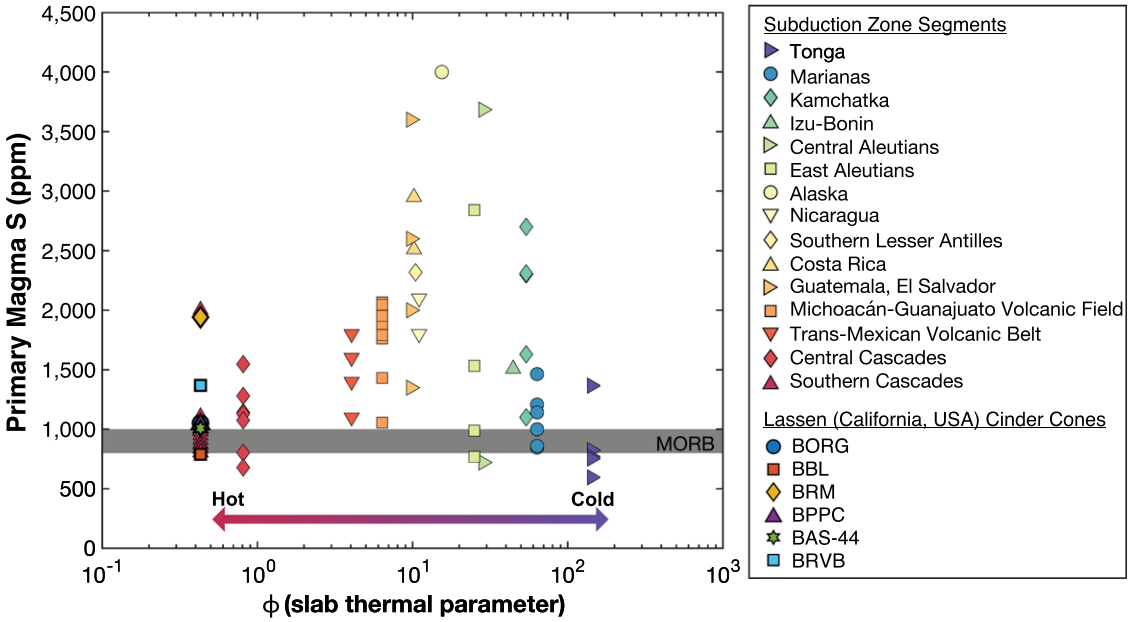

Figure 1. Calculated primary magma sulfur concentrations for arc volcanoes compared to the slab thermal parameter (an indicator of slab temperature) (Syracuse et al., 2010; Ruscitto et al., 2012; see the Supplemental Material [see footnote 1]). Primary mid-ocean ridge basalt (MORB) S reference values (Ding and Dasgupta, 2017) are shown for comparison. See Table S14 for locations of Lassen cinder cones.

Sr rather than Sr/Nd are stronger, with no outliers (Fig. S14), but we have chosen to retain Sr/Nd for modeling slab additions beneath Lassen for consistency with previous work (e.g., Walowski et al., 2016) and to reduce complications related to mantle melt fraction in our interpretations.

Correlations in Figure 2 and Figure S14 require variable slab addition of S to the mantle source and/or a variably oxidized mantle. With regard to the latter, MORB-source mantle that becomes oxidized without S addition does not contain enough S to generate the high-S magmas at Lassen (Fig. S13). An alternative is that magmas at each cinder cone became variably oxidized and S enriched during deep crustal differentiation. Theoretically, melt Fe^{3+} enrichment caused by magma recharge and garnet crystallization could increase $S^{6+}/\sum S$ and cause assimilation of sulfide cumulates in the lower crust (e.g., Lee and Tang, 2020). However, Lassen cinder cones are fed by small, short-lived crustal magmatic systems, and the high-Mg MIs used here formed during early crystallization. Lassen magmas also do not show the strong heavy rare earth element (HREE) depletions expected from protracted garnet fractionation (Walowski et al., 2016).

We therefore interpret correlations between S/Dy and Sr/Nd (Fig. 2D) to indicate that a large portion of S in Lassen magmas is sourced from the subducting slab. H_2O and Cl in Lassen magmas show similar patterns, indicating that S, Cl, and H_2O are all sourced primarily from the downgoing plate (Fig. S16; Walowski et al., 2016), consistent with volatiles in arcs globally (Ruscitto et al., 2012).

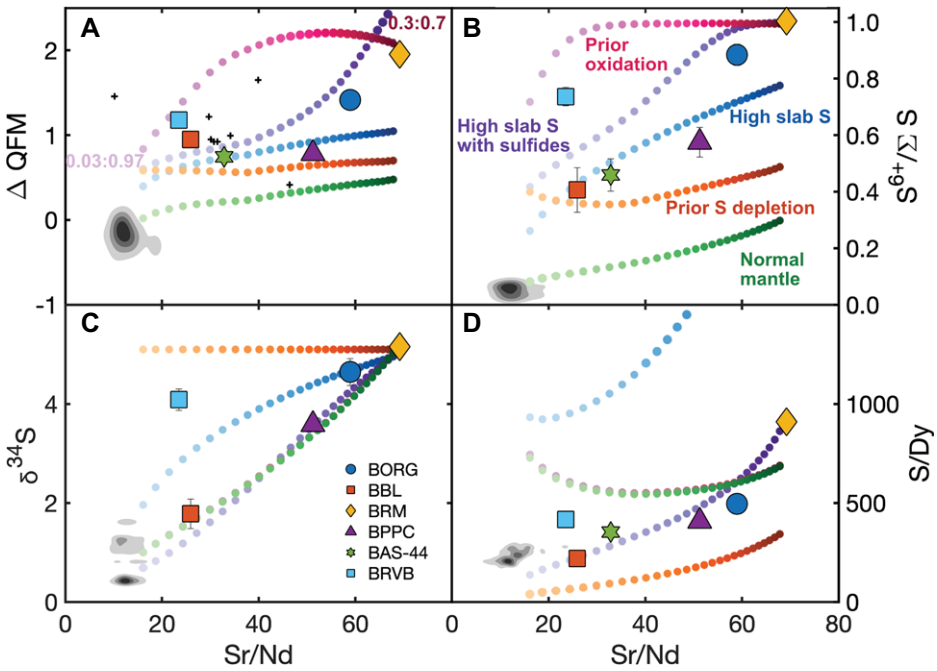

Figure 2. Primary magma compositions for the Lassen region (California, USA) based on melt inclusion data (from indicated cinder cones, large symbols; See Table S14 [see footnote 1] for locations of cinder cones) compared to model melt compositions (small circles). QFM—quartz-fayalite-magnetite. Error bars in B and C represent the standard error of the mean. Each array of colored circles represents one modeled scenario, and each individual circle represents modeled melt at peak mantle-wedge temperature, calculated for a specific melt/rock ratio, labeled next to the "Prior Oxidation" array in panel A as an example. "Normal mantle" and "Prior oxidation" models in C and D have the same values. See the text and Figure S3 for model details. Small crosses are oxygen fugacity estimates using spinel-olivine oxybarometry for other Lassen cinder cones (Ballhaus et al., 1991; Clynne and Borg, 1997). Mid-ocean ridge basalt compositions (Table S13) are shown in gray density contours for comparison. In D, the poor fit of three of the models to the data at low Sr/Nd is caused by the absence of residual sulfide (see Fig. S11).

SULFUR ISOTOPES

Because S/Dy can vary as a function of oxidation state during mantle melting, S isotope ratios ($\delta^{34}S$) measured in MIs provide an essential additional constraint on slab-to-mantle mass transfer of S. $\delta^{34}S$ values for Lassen magmas (1.8‰ ± 0.7‰ to 5.2‰ ± 0.3‰) correlate with Sr/Nd in a similar way to S/Dy ($R^2 = 0.68$, p-value = 0.04; Fig. 2C). This requires variable addition of high-$\delta^{34}S$ sulfur into a MORB-like mantle source ($\delta^{34}S = 0.6$‰; see the Supplemental Material). To compare $\delta^{34}S$ in Lassen magmas to $\delta^{34}S$ in slab lithologies, we calculate bulk $\delta^{34}S$ in the downgoing slab at Lassen using constraints from geophysical data and drill cores (Fig. 3; see the Supplemental Material). Our estimate includes sediments, volcanic and gabbroic sections of altered oceanic crust (AOC),

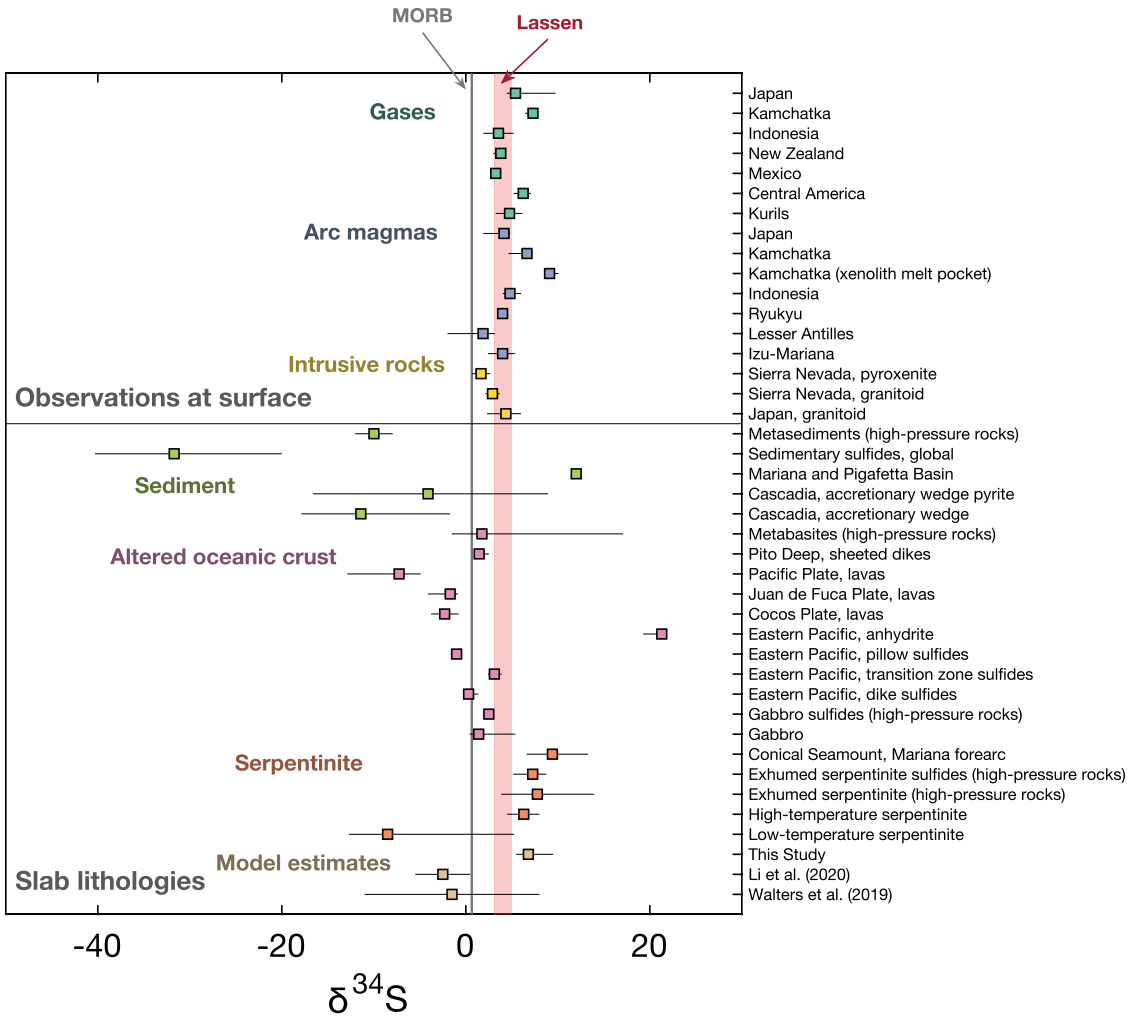

Figure 3. $\delta^{34}S$ values for arc volcanoes, drill cores, exhumed rocks, and slab fluid or melt models (see Table S11 for the values and the data sources [see footnote 1]). Symbols show the average and upper and lower quartiles for each data set. All data are for whole-rock S unless otherwise specified. Arc extrusive rocks ("Arc magmas") include basalt and basaltic andesite compositions. Average mid-ocean ridge basalt (MORB) $\delta^{34}S$ and the upper and lower quartile of Lassen (California, USA) melt inclusion $\delta^{34}S$ are shown for comparison.

and 2 km of partially hydrated lithospheric mantle. Bulk $\delta^{34}S$ estimated for the slab beneath Lassen is $-6.7‰ \pm 2.9‰$, with uncertainty based on S content in each section. Sediment contribution to the slab-derived component in Lassen magmas is small (Walowski et al., 2016). If we exclude sediment, bulk slab $\delta^{34}S$ is $1.1‰ \pm 0.5‰$, still lower than $\delta^{34}S$ in the most S-rich Lassen cinder cone ($\delta^{34}S = 5.2‰$) and indistinguishable from that in MORB ($\delta^{34}S = 0.6‰$).

Elevated $\delta^{34}S$ in Lassen magmas relative to estimates for the bulk downgoing slab (Figs. 2 and 3) could be most readily explained if seawater sulfate in downgoing hydrated lithospheric mantle or AOC was transported into the sub-arc mantle more effectively than sulfur from primary sulfides in downgoing AOC. Heterogeneity in sulfide $\delta^{34}S$ within exhumed high-pressure rocks suggests sulfides do not equilibrate efficiently at slab surface temperatures (Walters et al., 2019). If this were the case, then $\delta^{34}S$-enriched fluids from hydrated lithospheric mantle (e.g., Alt et al., 2012) that flush overlying oceanic crust and cause partial melting would have a disproportionate effect on slab melt $\delta^{34}S$. Alternatively, if equilibrium conditions prevailed, slab sulfur may inherit high $\delta^{34}S$ from isotopic fractionation during slab melting. An S^{6+}-dominated slab melt in equilibrium with MORB-like sulfides ($\delta^{34}S = 0‰$) would have $\delta^{34}S = 5.7‰$–$6.9‰$ (Miyoshi et al., 1984) at 750–850 °C (Walowski et al., 2015), whereas a S^{2-}-dominated slab melt would undergo little fractionation. For partial melt of oceanic crust to be dominated by S^{6+} requires that fluids derived from underlying hydrated mantle lithosphere be relatively oxidized (e.g., Debret and Sverjensky, 2017; Maurice et al., 2020, Evans and Frost, 2021). Therefore, while assumptions about equilibrium or nonequilibrium $\delta^{34}S$ behavior in AOC have different implications for the precise source of slab S, both indicate the release of oxidized, S^{6+}-dominated melt from the slab into the mantle wedge.

Values of $\delta^{34}S$ in Lassen MIs are similar to $\delta^{34}S$ measured at arcs globally (Fig. 3). High-temperature gases, low-S submarine glasses, and degassed scoria samples all have $\delta^{34}S$ similar to that of the minimally degassed MIs measured here. This suggests that degassing at arcs has a relatively small effect on melt $\delta^{34}S$ values. Considering the wide range of sediment $\delta^{34}S$ compositions (Fig. 3), slab temperatures (Syracuse et al., 2010), and slab-material fluxes (Ruscitto et al., 2012) estimated for arcs, similarities in $\delta^{34}S$ of magmas from different arcs suggest that the addition of slab-derived, oxidized S to the sub-arc mantle at Lassen is common to other subduction zones.

INFLUENCE OF SLAB-DERIVED SULFUR ON THE OXIDATION STATE OF LASSEN MAGMAS

Lassen primary magma oxygen fugacities (f_{O2}) relative to the quartz-fayalite-magnetite (QFM) buffer, calculated from $Fe^{3+}/\sum Fe$ measured in MIs, range from QFM + 0.8 to QFM + 2.0 (Fig. 2A; see the Supplemental Material). Like S and $\delta^{34}S$, f_{O2} correlates with Sr/Nd ($R^2 = 0.61$, p-value = 0.04 for ΔQFM, $R^2 = 0.68$, p-value = 0.02 for $S^{6+}/\sum S$), suggesting that slab-derived S^{6+} has a causal link to oxidized magmas. Both $Fe^{3+}/\sum Fe$ and $S^{6+}/\sum S$ are elevated relative to MORB. This requires that as slab-derived, hydrous, silicic melt causes flux melting of the mantle wedge (Walowski et al., 2015), a portion of slab-derived S^{6+} is reduced to oxidize Fe^{2+}, given that there is an equilibrium relationship between melt $Fe^{3+}/\sum Fe$ and $S^{6+}/\sum S$ involving redox exchange between S and Fe (e.g., Nash et al., 2019). Therefore, to assess whether slab-derived S^{6+} causes arc magmas to be more oxidized than MORB, the coupled redox budget of S and Fe must be considered.

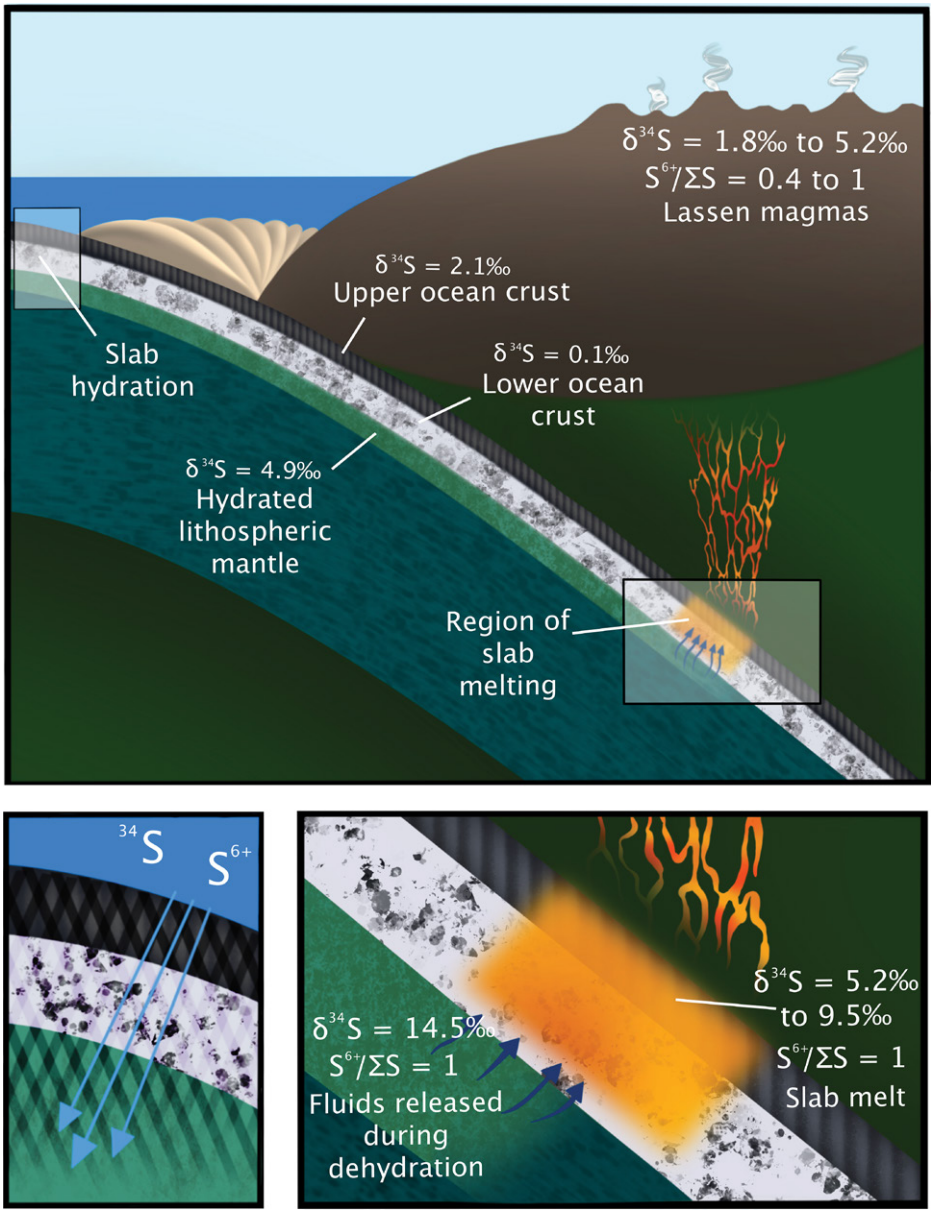

Figure 4. Conceptual model for the generation of sulfur-rich oxidized magmas in the southern Cascade arc. High-$\delta^{34}S$ seawater sulfate (e.g., Alt et al., 2012) becomes incorporated into altered oceanic crust (subdivided into upper crust with both volcanic rocks and sheeted dikes, and lower crust with gabbros) and hydrated mantle lithosphere during hydrothermal activity near the ridge crest and later faulting of the oceanic crust. When hydrated mantle lithosphere dehydrates, oxidized fluids rise into the overlying oceanic crust, generating high-$\delta^{34}S$, sulfate-dominated, hydrous slab melts. These slab melts rise up through the inverted thermal gradient of the mantle wedge, reacting with mantle peridotite to form oxidized, S-rich, high-$\delta^{34}S$ basaltic magmas. Inset panels show details of slab hydration and slab melting.

To model the redox budget, we combine pMELTS melting models (Ghiorso et al., 2002), redox equilibrium between S and Fe, and electron balance calculations. This model (see the Supplemental Material for details) approximates the reaction and transport of silicic, hydrous slab melts rising into the inverted thermal gradient of the mantle wedge (Sisson and Kelemen, 2018). Coupled redox balance calculations track changes in $Fe^{3+}/\sum Fe$ and $S^{6+}/\sum S$ during reactions of S^{6+}-rich slab-derived melts with more reduced mantle peridotite. Importantly, the coupled redox balance shows that slab S^{6+} is much less effective at generating oxidized basaltic magmas than predicted when only the relationship between f_{O_2} and $S^{6+}/\sum S$ is considered (Klimm et al., 2012).

In our initial model, we assume a slab melt with 1500 ppm S^{6+} based on a 950 °C, 3 GPa partial melting experiment of oxidized, fluid-saturated, S-rich basalt (Jégo and Dasgupta, 2014) and initial mantle peridotite S^{2-} content of 150 ppm based on MORB-source mantle (Ding and Dasgupta, 2017). In this scenario, slab S^{6+} drives clear increases in the f_{O_2} and $S^{6+}/\sum S$ of mantle melts but does not predict Lassen f_{O_2}, S/Dy, or $S^{6+}/\sum S$ values (green curve in Fig. 2). Given this result, we also modeled the same scenario but assumed 10,000 ppm S^{6+} in slab melt. This model overestimates the S content of Lassen magmas but reproduces all but the highest Lassen f_{O_2} and $S^{6+}/\sum S$ values (blue curve in Fig. 2). Given that this modeling approach seems to require unreasonably high slab melt S^{6+} concentrations, we explored three more-complex model scenarios.

In the first more-complex scenario, melts remain saturated in an immiscible sulfide phase as they react with peridotite. This model scenario creates more oxidizing mantle melts but requires very S-rich slab melt (8000 ppm) to reproduce the highest f_{O_2} and $S^{6+}/\sum S$ values (purple curve in Fig. 2). The second more-complex scenario is that the sub-arc mantle experienced S extraction during previous melting events. However, if we assume 1500 ppm S^{6+} in slab melt and 0 ppm S^{2-} in mantle peridotite, the model cannot reproduce higher f_{O_2} and S/Dy values or the correlation between Sr/Nd and $\delta^{34}S$ (orange curve in Fig. 2). The third more-complex scenario is that the sub-arc mantle experienced multiple stages of oxidation, consistent with oxygen isotope data for Lassen magmas (Underwood and Clynne, 2017) and other arcs (Auer et al., 2009). This model fails to reproduce the entire range of Lassen compositions with a single, uniform period of prior oxidation (pink curve in Fig. 3), indicating that a more localized and/or multistage process is required.

Our models show that transfer of slab-derived sulfate to the mantle wedge has a clear effect on the f_{O_2} of arc magmas and requires slab melts with $\delta^{34}S = 5.2‰–9.5‰$ to match measured $\delta^{34}S$ values (Figs. 2, 3, and 4). These models highlight the importance of resolving sensitivity of S and Fe redox exchange to pressure, temperature, melt composition (including dissolved H_2O), and potential quenching effects (e.g., Matjuschkin et al., 2016; O'Neill, 2021). While these uncertainties are unlikely to alter bulk electron exchange in our models significantly compared to the overall effect of S^{6+} addition, they limit how modeling outcomes considered here can be included in models of S behavior during mantle melting.

A striking feature of our data set is that Lassen magma $\delta^{34}S$ and f_{O_2} values are similar to those measured in the Mariana Islands (western Pacific Ocean) (Fig. S6; Alt et al., 1993; Brounce et al., 2014) and other arcs globally (Fig. 3; Cottrell et al., 2020) even though the Cascade arc is a near-global end member in terms of young slab age and temperature, which strongly affect slab dehydration and melting (Walowski et al., 2015). This shared similarity in $\delta^{34}S$ and f_{O_2} points to a common source of S, either sulfate derived from hydrated mantle lithosphere or AOC-hosted sulfides oxidized by fluids rising up from the hydrated mantle lithosphere, or both (Fig. 4). Our results show that transfer of slab-derived S^{6+} into sub-arc mantle above

subducted plates can explain both elevated $\delta^{34}S$ values and f_{O_2} of basaltic arc magmas globally.

ACKNOWLEDGMENTS

We thank K. Walowski and M. Clynne for sampling assistance and helpful discussions; A. Lanzirotti, M. Newville, B. Monteleone, C. Russo, A. Kent, J. Donovan, and J. Andrys for analytical assistance; and K. Tate-Jones for conceptual model illustrations. We thank M. Brounce and two anonymous reviewers for their constructive reviews of this manuscript. This material is based upon work supported by the U.S. National Science Foundation (NSF) Graduate Research Fellowship under grant 1842486. Portions of this work were performed at GeoSoilEnviroCARS (The University of Chicago, Sector 13), Advanced Photon Source (APS), Argonne National Laboratory (Lemont, Illinois, USA). GeoSoilEnviroCARS is supported by the NSF (grant EAR-1634415) and U.S. Department of Energy (DOE)–GeoSciences (grant DE-FG02-94ER14466). This research used resources of APS, a DOE Office of Science User Facility operated for the DOE Office of Science by Argonne National Laboratory under contract DE-AC02-06CH11357.

REFERENCES CITED

Alt, J.C., Shanks, W.C., III, and Jackson, M.C., 1993, Cycling of sulfur in subduction zones: The geochemistry of sulfur in the Mariana Island Arc and back-arc trough: Earth and Planetary Science Letters, v. 119, p. 477–494, https://doi.org/10.1016/0012-821X(93)90057-G.

Alt, J.C., Garrido, C.J., Shanks, W.C., III, Turchyn, A., Padrón-Navarto, J.A., Sánchez-Vizcaíno, V.L., Pugnaire, M.T.G., and Marchesi, C., 2012, Recycling of water, carbon, and sulfur during subduction of serpentinites: A stable isotope study of Cerro del Almirez, Spain: Earth and Planetary Science Letters, v. 327, p. 50–60, https://doi.org/10.1016/j.epsl.2012.01.029.

Auer, S., Bindeman, I., Wallace, P., Ponomareva, V., and Portnyagin, M., 2009, The origin of hydrous, high-$\delta^{18}O$ voluminous volcanism: Diverse oxygen isotope values and high magmatic water contents within the volcanic record of Klyuchevskoy volcano, Kamchatka, Russia: Contributions to Mineralogy and Petrology, v. 157, p. 209–230, https://doi.org/10.1007/s00410-008-0330-0.

Ballhaus, C., Berry, R.F., and Green, D.H., 1991, High-pressure experimental calibration of the olivine-orthopyroxene-spinel oxygen geobarometer: Implications for the oxidation state of the upper mantle: Contributions to Mineralogy and Petrology, v. 107, p. 27–40, https://doi.org/10.1007/BF00310615.

Bénard, A., Klimm, K., Woodland, A.B., Arculus, R.J., Wilke, M., Botcharnikov, R.E., Shimizu, N., Nebel, O., Rivard, C., and Ionov, D.A., 2018, Oxidising agents in sub-arc mantle melts link slab devolatilisation and arc magmas: Nature Communications, v. 9, 3500, https://doi.org/10.1007/BF00311183.

Birner, S.K., Warren, J.M., Cottrell, E., Davis, F.A., Kelley, K.A., and Falloon, T.J., 2017, Forearc peridotites from Tonga record heterogeneous oxidation of the mantle following subduction initiation: Journal of Petrology, v. 58, p. 1755–1780, https://doi.org/10.1093/petrology/egx072.

Borg, L.E., Clynne, M.A., and Bullen, T.D., 1997, The variable role of slab-derived fluids in the generation of a suite of primitive calc-alkaline lavas from the southernmost Cascades, California: Canadian Mineralogist, v. 35, p. 425–452.

Brounce, M.N., Kelley, K.A., and Cottrell, E., 2014, Variations in $Fe^{3+}/\Sigma Fe$ of Mariana arc basalts and mantle wedge fO_2: Journal of Petrology, v. 55, p. 2513–2536, https://doi.org/10.1093/petrology/egu065.

Clynne, M.A., and Borg, L.E., 1997, Olivine and chromian spinel in primitive calc-alkaline and tholeiitic lavas from the southernmost Cascade Range, California: A reflection of relative fertility of the source: Canadian Mineralogist, v. 35, p. 453–472.

Cottrell, E., Birner, S., Brounce, M., David, F., Waters, L.E., and Kelley, K.A., 2020, Oxygen fugacity across tectonic settings, *in* Neuville, D.R. and Moretti, R. eds., Redox: Variables and Mechanisms in Magmatism and Volcanism: American Geophysical Union Geophysical Monograph, https://doi.org/10.1002/9781119473206.ch3.

Debret, B., and Sverjensky, D.A., 2017, Highly oxidising fluids generated during serpentinite breakdown in subduction zones: Scientific Reports, v. 7, 10351, https://doi.org/10.1038/s41598-017-09626-y.

Ding, S., and Dasgupta, R., 2017, The fate of sulfide during decompression melting of peridotite—Implications for sulfur inventory of the MORB-source depleted upper mantle: Earth and Planetary Science Letters, v. 459, p. 183–195, https://doi.org/10.1016/j.epsl.2016.11.020.

Evans, K.A., 2012, The redox budget of subduction zones: Earth-Science Reviews, v. 113, p. 11–32, https://doi.org/10.1016/j.earscirev.2012.03.003.

Evans, K.A., and Frost, B.R., 2021, Deserpentinization in subduction zones as a source of oxidation in arcs: A reality check: Journal of Petrology, v. 62, egab016, https://doi.org/10.1093/petrology/egab016.

Ghiorso, M.S., Hirschmann, M.M., Reiners, P.W., and Kress, V.C., 2002, The pMELTS: A revision of MELTS for improved calculation of phase relations and major element partitioning related to partial melting of the mantle to 3 GPa: Geochemistry Geophysics Geosystems, v. 3, p. 1–35, https://doi.org/10.1029/2001GC000217.

Jégo, S., and Dasgupta, R., 2014, The fate of sulfur during fluid-present melting of subducting basaltic crust at variable oxygen fugacity: Journal of Petrology, v. 55, p. 1019–1050, https://doi.org/10.1093/petrology/egu016.

Kelley, K.A., and Cottrell, E., 2009, Water and the oxidation state of subduction zone magmas: Science, v. 325, p. 605–607, https://doi.org/10.1126/science.1174156.

Klimm, K., Kohn, S.C., and Botcharnikov, R.E., 2012, The dissolution mechanism of sulphur in hydrous silicate melts.II: Solubility and speciation of sulphur in hydrous silicate melts as a function of fO_2: Chemical Geology, v. 322–323, p. 250–267, https://doi.org/10.1016/j.chemgeo.2012.04.028.

Lee, C.-T.A., and Tang, M., 2020, How to make porphyry copper deposits: Earth and Planetary Science Letters, v. 529, 115868, https://doi.org/10.1016/j.epsl.2019.115868.

Lee, C.-T.A., Luffi, P., Le Roux, V., Dasgupta, R., Albaréde, F., and Leeman, W.P., 2010, The redox state of arc mantle using Zn/Fe systematics: Nature, v. 468, p. 681–685, https://doi.org/10.1038/nature09617.

Li, J.L., Schwarzenbach, E.M., John, T., Ague, J.J., Huang, F., Gao, J., Klemd, R., Whitehouse, M.J., and Wang, X.S., 2020, Uncovering and quantifying the subduction zone sulfur cycle from the slab perspective: Nature Communications, v. 11, https://doi.org/10.1038/s41467-019-14110-4.

Matjuschkin, V., Blundy, J.D., and Brooker, R.A., 2016, The effect of pressure on sulphur speciation in mid- to deep-crustal arc magmas and implications for the formation of porphyry copper deposits: Contributions to Mineralogy and Petrology, v. 171, 66, https://doi.org/10.1007/s00410-016-1274-4.

Maurice, J., Bolfan-Casanova, N., Demouchy, S., Chauvigne, P., Schiavi, F., and Debret, B., 2020, The intrinsic nature of antigorite breakdown at 3 GPa: Experimental constraints on redox conditions of serpentinite dehydration in subduction zones: Contributions to Mineralogy and Petrology, v. 175, 94, https://doi.org/10.1007/s00410-020-01731-y.

Miyoshi, T., Sakai, H., and Chiba, H., 1984, Experimental study of sulfur isotope fractionation factors between sulfate and sulfide in high temperature melts: Geochemical Journal, v. 18, p. 75–84, https://doi.org/10.2343/geochemj.18.75.

Nash, W.M., Smythe, D.J., and Wood, B.J., 2019, Compositional and temperature effects on sulfur speciation and solubility in silicate melts: Earth and Planetary Science Letters, v. 507, p. 187–198, https://doi.org/10.1016/j.epsl.2018.12.006.

O'Neill, H.St.C., 2021, Comment on "Compositional and temperature effects on sulfur speciation and solubility in silicate melts" by Nash et al. [Earth and Planet. Sci. Lett. 507 (2019) 187–198]: Earth and Planetary Science Letters, v. 560, 116843, https://doi.org/10.1016/j.epsl.2021.116843.

Richards, J.P., 2015, The oxidation state, and sulfur and Cu contents of arc magmas: Implications for metallogeny: Lithos, v. 233, p. 27–45, https://doi.org/10.1016/j.lithos.2014.12.011.

Ruscitto, D.M., Wallace, P.J., Cooper, L.B., and Plank, T., 2012, Global variations in H_2O/Ce: 2. Relationships to arc magma geochemistry and volatile fluxes: Geochemistry Geophysics Geosystems, v. 13, Q03025, https://doi.org/10.1029/2011GC003887.

Saal, A.E., Hauri, E.H., Langmuir, C.H., and Perfit, M.R., 2002, Vapour undersaturation in primitive mid-ocean-ridge basalt and the volatile content of Earth's upper mantle: Nature, v. 419, p. 451–455, https://doi.org/10.1038/nature01073.

Sisson, T.W., and Kelemen, P.B., 2018, Near-solidus melts of MORB + 4 wt% H_2O at 0.8–2.8 GPa applied to issues of subduction magmatism and continent formation: Contributions to Mineralogy and Petrology, v. 173, 70, https://doi.org/10.1007/s00410-018-1494-x.

Syracuse, E.M., van Keken, P.E., and Abers, G.A., 2010, The global range of subduction zone thermal models: Physics of the Earth and Planetary Interiors, v. 183, p. 73–90, https://doi.org/10.1016/j.pepi.2010.02.004.

Tang, M., Erdmann, M., Eldridge, G., and Lee, C.-T.A., 2018, The redox "filter" beneath magmatic orogens and the formation of continental crust: Science Advances, v. 4, eaar4444, https://doi.org/10.1126/sciadv.aar4444.

Underwood, S.J., and Clynne, M.A., 2017, Oxygen isotope geochemistry of mafic phenocrysts in primitive mafic lavas from the southernmost Cascade Range, California: American Mineralogist, v. 102, p. 252–261, https://doi.org/10.2138/am-2017-5588.

Walowski, K.J., Wallace, P.J., Hauri, E.H., Wada, I., and Clynne, M.A., 2015, Slab melting beneath the Cascade Arc driven by dehydration of altered oceanic peridotite: Nature Geoscience, v. 8, p. 404–408, https://doi.org/10.1038/ngeo2417.

Walowski, K.J., Wallace, P.J., Clynne, M.A., Rasmussen, D.J., and Weis, D., 2016, Slab melting and magma formation beneath the southern Cascade arc: Earth and Planetary Science Letters, v. 446, p. 100–112, https://doi.org/10.1016/j.epsl.2016.03.044.

Walters, J.B., Cruz-Uribe, A.M., and Marschall, H.R., 2019, Isotopic compositions of sulfides in exhumed high-pressure terranes: Implications for sulfur cycling in subduction zones: Geochemistry Geophysics Geosystems, v. 20, p. 3347–3374, https://doi.org/10.1029/2019GC008374.

Printed in USA